Available online at www.sciencedirect.com
SCIENCE DIRECT
Journal of Catalysis 238 (2006) 153–164
JOURNAL OF CATALYSIS
www.elsevier.com/locate/jcat

Selectivity changes during organic photooxidation on TiO_2: Role of O_2 pressure and organic coverage

M.A. Henderson [a,*], J.M. White [a,1], H. Uetsuka [b,2], H. Onishi [b,3]

[a] *Institute for Interfacial Catalysis, Pacific Northwest National Laboratory, PO Box 999, MS K8-93 Richland, WA 99352, USA*
[b] *Surface Chemistry Laboratory, Kanagawa Academy of Science and Technology, KSP Sakado, Takatsu, Kawasaki, 213-0012 Japan*

Received 26 July 2005; revised 29 November 2005; accepted 3 December 2005

Available online 9 January 2006

Abstract

The selectivity of trimethyl acetate (TMA) photodecomposition on TiO_2(110) as a function of O_2 pressure and TMA coverage was probed at room temperature (RT) using isothermal mass spectrometry (ISOMS) and scanning tunneling microscopy (STM). The selectivity of TMA photodecomposition on TiO_2(110) is sensitive to the initial TMA coverage and O_2 pressure. TMA bridge-bonds to the surface via the carboxylate end of the molecule in a manner consistent with the binding of other carboxylate species (e.g., formate and acetate) on TiO_2 surfaces. Under all conditions, photodecomposition of TMA was initiated via hole reaction with the electron in carboxylate's π system, resulting in opening of the O–C–O bond angle and formation of CO_2 and a *t*-butyl radical by cleavage of the C–C bond between these groups. The CO_2 product desorbs from the surface at RT, but the *t*-butyl radical has several options for thermal chemistry. In ultrahigh vacuum (UHV), where the O_2 partial pressure is $< 1 \times 10^{-10}$ Torr, the TMA photodecomposition results in a near 1:1 yield of isobutene (*i*-C_4H_8) and isobutane (*i*-C_4H_{10}) from surface chemistry of the *t*-butyl radicals. STM results show that the reaction occurs fairly homogeneously across the TiO_2(110) surface. In the presence of O_2, the photodecomposition selectivity switches from initially *i*-C_4H_8 to a mixture of *i*-C_4H_8 and *i*-C_4H_{10} and then back to predominately *i*-C_4H_8. The latter selectivity change occurs at the point at which void regions form and grow in the TMA overlayer. At this point, the photodecomposition rate accelerates and the reaction occurs preferentially at the interface between the TMA-rich and TMA-void regions on the surface. These results illustrate both the changing dynamics of a typical photooxidation reaction on TiO_2 and also how factors such as O_2 pressure and TMA coverage impact the photooxidation reaction selectivity. We also present results that suggest the rate of photodecomposition of monodentate carboxylates is greater than that of bidentate (bridging) carboxylates. This implies that the structural arrangement of Ti cation sites on the surface is an important issue that influences photocatalytic rates on TiO_2.

Keywords: TiO_2; TiO_2(110); Trimethyl acetate; Photocatalysis; Photooxidation; Reaction selectivity; STM; Mass spectrometry

1. Introduction

Photocatalysis on TiO_2 [1–4] continues to be a growing area of catalytic research due to potential applications such as wastewater treatment, air purification, self-cleaning and disinfecting surfaces, and water splitting. Using the rutile TiO_2(110) surface as a model photocatalyst, we recently published a series of papers [5–9] exploring some of the fundamental aspects of photocatalysis on TiO_2. The adsorbate trimethyl acetic acid (TMAA) has been a convenient probe molecule in these studies because, along with other molecules in the carboxylic acid classification (e.g., formic and acetic acids), it adsorbs on TiO_2 surface to yield strongly bound carboxylate species [10]. These organic carboxylates on TiO_2(110) have fairly well-understood adsorption structures and thermal chemistries, and in the case of trimethyl acetate (TMA) have reasonably high photoreactivity when exposed to UV light. TMAA adsorbs dissociatively on

* Corresponding author. Fax: +1 509 376 2192.
E-mail address: ma.henderson@pnl.gov (M.A. Henderson).
[1] Visiting professor from the Department of Chemistry and Biochemistry, University of Texas, Austin, TX 78712, USA.
[2] Current address: Technology Research and Development Department, General Technology Division, Central Japan Railway Company, Komaki, 485-0801, Japan.
[3] Current address: Department of Chemistry, Faculty of Science, Kobe University, Kobe 657-8501, Japan.

0021-9517/$ – see front matter
doi:10.1016/j.jcat.2005.12.004

TiO_2(110) at 300 K (hereinafter referred to as room temperature [RT]) by cleavage of the molecule's O–H bond. The carboxylate group (TMA) bridge-bonds across two Ti^{4+} sites, with the molecular plane oriented normal to the surface and along the row of Ti^{4+} sites (the <001> surface crystallographic direction). The acid proton adsorbs on a bridging O^{2-} site, forming a bridging OH group. As shown in the following reactions, the initial step in the photodecomposition of TMA on TiO_2(110) involves a hole reaction with the carboxylate group to generate CO_2 and a *t*-butyl radical:

$$TiO_2 + h\nu \rightarrow h^+ + e^-, \quad (1)$$

$$TMA + h^+ \rightarrow CO_{2(g)} + t\text{-butyl}_{(a)}, \quad (2)$$

where h^+ and e^- are the resulting hole in the TiO_2 valence band and the excited electron in the TiO_2 conduction band, respectively. The designations "a" and "g" refer to adsorbed and gaseous species, respectively. Reaction (2) resembles the Hunsdiecker [11] and "photo-Kolbe" [12,13] reactions known for decarboxylation of organic acids. Excited electrons are trapped at surface cations that bind bridging OH groups [6,14–16]. These OH groups react with O_2 according to the following reactions:

$$Ti^{4+}\text{–}OH^-\text{–}Ti^{4+} + e^- \rightarrow Ti^{4+}\text{–}OH^-\text{–}Ti^{3+}, \quad (3)$$

$$Ti^{4+}\text{–}OH^-\text{–}Ti^{3+} + O_2 \rightarrow Ti^{4+}\text{–}O^{2-}\text{–}Ti^{4+} + \{OOH\}. \quad (4)$$

The OOH species is speculative in this case (although related species have been observed under other conditions [17–19]), because the observable products of reaction (4) are O adatoms and OH groups, the latter of which disproportionate to water at RT [16,20]. Returning to reaction (2), the mechanism of TMA photodecomposition on TiO_2(110) in the absence of O_2 has been reported [9]. Experiments in which TMA was irradiated with UV light at 100 K permitted subsequent identification of products using TPD. Photogenerated CO_2 desorbed from TiO_2(110) at ∼150 K and exhibited no additional reactivity with the surface on heating or when photolysis was performed at RT. If produced at 100 K, the *t*-butyl radicals adsorb intact on the TiO_2(110) surface and react on heating. If produced at RT, they undergo rapid thermal reactions yielding gaseous isobutene and isobutane,

$$2t\text{-Butyl}_{(a)} \rightarrow i\text{-}C_4H_{8(g)} + i\text{-}C_4H_{10(g)}. \quad (5)$$

Isobutene (i-C_4H_8) and isobutane (i-C_4H_{10}) both thermally desorb from TiO_2(110) at temperatures well below RT, so these products are liberated from the surface at RT on formation.

In this study, isothermal mass spectrometry (ISOMS) and scanning tunneling microscopy (STM) were used to study the influence of O_2 on TMA photodecomposition and on the selectivity between the isobutene and isobutane products. In a sustained photooxidation reaction that results in complete conversion of the organic in question, the photooxidation mechanisms of secondary products, such as isobutene and isobutane, may well dictate the overall kinetics of the process. Therefore, factors that influence the selectivity of the primary photooxidation event [in this case, the coupled reactions (2), (4), and (5)] may significantly impact the entire photooxidation process. For example, the adsorption energy of isobutene on TiO_2(110) is slightly greater than that of isobutane [9], so under reaction conditions one would expect that an isobutane molecule would be more easily displaced from the surface and thus less able to compete for adsorption and reaction sites. Additionally, the kinetics of isobutene photooxidation should be different than those of isobutane if only in the sense that the latter will require an additional oxidative step in the process of complete photooxidation.

We show that the selectivity of the initial step in TMA photooxidation on TiO_2(110) is sensitive to the O_2 pressure and the surface coverage of TMA. In UHV, adsorbed TMA photodecomposition is spatially homogeneous on the surface and yields a near-stoichiometric mixture of isobutene and isobutane. As the O_2 pressure is increased, the photooxidation reaction shifts to a spatially nonhomogeneous process based on STM data. Nonhomogeneity is exhibited in STM by fairly well separated hydrophilic (possessing adsorbed water, OH, and O_x) and hydrophobic (possessing unreacted TMA) regions. Under these conditions, the photooxidation of TMA occurs preferentially at the boundary of the two regions, yielding predominantly isobutene. The overall rate of the reaction accelerates as the hydrophilic regions expand, allowing unimpeded access of O_2 to the surface [7].

2. Experimental

The ultrahigh-vacuum (UHV) system used for the ISOMS measurements in this study has a base pressure of 2×10^{-10} Torr. The TiO_2(110) crystal (10 × 10 × 1.5 mm) was the same as used in previous studies of TMAA on TiO_2(110) [6–10], and the same sample cleaning preparations were used in this study. Briefly, the sample was cleaned by ion bombardment followed by annealing in UHV at 850 K. Sample cleanliness and surface order were monitored using AES and LEED, respectively. TMAA (Aldrich, research grade) is a solid at RT with a vapor pressure of about 0.5 Torr. The TMAA source was purified initially by freeze–pump–thaw cycles using a liquid nitrogen (LN2) bath, but also with a melting step using a hot water bath followed by pumping on the liquid to remove any gaseous impurities in the solid TMAA. TMAA was dosed on the crystal using a pinhole apertured directional doser. The inner diameter of the doser was about 5 mm so that the crystal could be preferentially exposed to TMAA without exposing the sample holder. Research-grade oxygen was further purified by passing the gas through a LN2 trap to remove condensable impurities. Oxygen exposure was accomplished by backfilling the chamber through a leak valve.

Isothermal mass spectrometry (ISOMS) and temperature-programmed desorption (TPD) were performed with the same quadrupole mass spectrometer (QMS). TPD, performed with a heating rate of 2 K/s between 95 and 750 K, was used primarily to determine adsorbate coverage. Thorough TPD studies of TMAA on TiO_2(110) with and without UV irradiation can be found elsewhere [9,10]. In ISOMS, a series of masses were tracked as function of time at a set crystal temperature. All such experiments were performed with the crystal at RT. The crys-

tal was positioned in front of the QMS so that UV light was incident. This placed the crystal normal direction at a 45° angle from the entrance cone to the mass spectrometer. A typical experiment involved dosing the crystal with TMAA, followed by stabilizing a background pressure of O_2. Background levels of selected masses were established in the dark for reasonable baselines, and then the crystal was exposed to UV light for a desired period. ISOMS experiments were terminated by blocking the UV light and reestablishing baseline background signals. UV light from a 100 W Hg arc lamp was directed through a sapphire viewport and focused down to an area covering the entire crystal face. Given that TMAA was exposed exclusively on the TiO_2(110) crystal face (see above), background photodesorption signals from noncrystal surfaces were negligible. The photon flux was calibrated using a photodiode detector.

As discussed previously, the ISOMS signals were calibrated to flux units of monolayers per second using calibration signals from TPD of known coverages of TMAA, isobutene, isobutane, and water on TiO_2(110) [9,10,21]. One monolayer is defined as the surface cation density on the ideal TiO_2(110) surface (5.2×10^{14} cm^{-2}). Included in the calibration was a normalization factor to account for the different sample orientations in the ISOMS and TPD positions.

STM studies were conducted in a separate chamber using a JEOL JSPM-4500S microscope as described previously. The TiO_2(110) crystal used in these measurements was treated in much the same manner as in the ISOMS measurements. Photolysis measurements in this chamber used a 300 W Xe arc lamp. Because the UV output of this lamp was about 8 times less than that of the 100 W Hg arc lamp used in the ISOMS measurements, the irradiation times used in the two measurements cannot be compared directly.

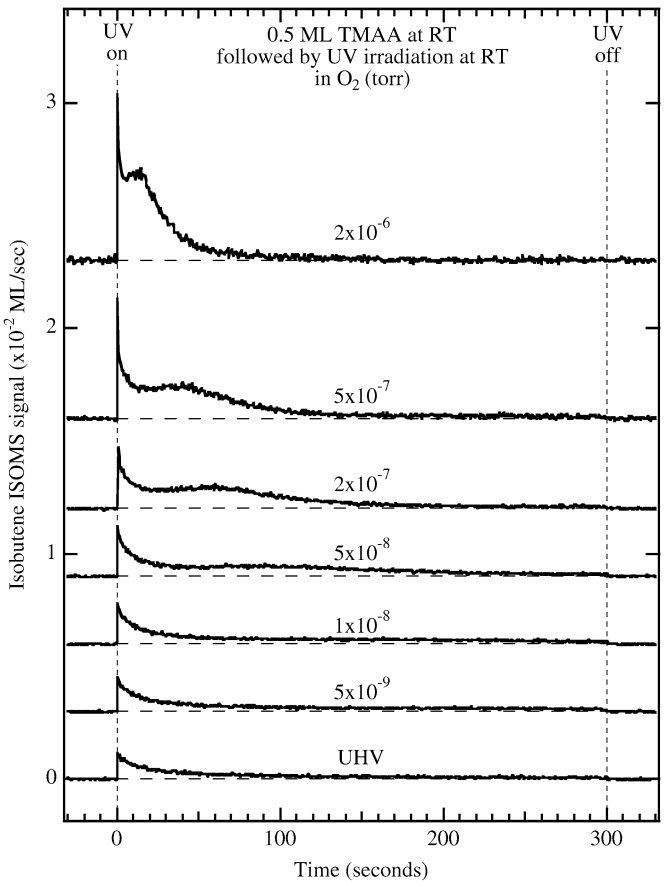

Fig. 1. Isobutene ISOMS scans from UV irradiation of 0.5 ML TMA on TiO_2(110) at RT in various background pressures of O_2. UV irradiation was commenced at time 0 s and was terminated at time 300 s. UV irradiation was with a 100 W Hg lamp. Spectra are displaced vertically and provided with background lines for clarity.

3. Results and discussion

3.1. Effect of O_2 pressure on the selectivity of TMA photodecomposition

Fig. 1 shows isobutene ISOMS traces from UV irradiation of 0.5 ML TMA on TiO_2(110) in various background pressures of O_2. At this coverage, the TMA adlayer formed a well-ordered (2 × 1) structure [6–8] (see below) in which virtually all of the TMA groups were bound in an η^2 bridge-bonded configuration [22]. In each experiment, isobutene desorption signal was registered immediately on exposure of the surface to UV light (designated as time "0") and continued to varying extents as the light was maintained. Typically, sharp rises in various ISOMS signals were observed on the initial exposure of the surface to UV. These sharp signal rises are hereinafter referred to as "spikes." In UHV (bottom trace), the isobutene ISOMS signal abruptly rose on exposure of the 0.5 ML TMA surface to UV, but decayed thereafter. The isobutene ISOMS profile did not significantly change for increasing O_2 pressures up to 1×10^{-8} Torr, but two noteworthy changes occurred above this pressure. First, the initial isobutene ISOMS rate (the spike) increased with increasing O_2 pressure, and second, a "hump" in the rate of isobutene evolution developed later, reflective of an increased TMA photodecomposition rate. The hump was broadly distributed in time for an O_2 pressure of 5×10^{-8} Torr, but narrowed and shifted toward shorter times as the O_2 pressure was increased. Maintaining vacuum integrity placed an upper limit of $\sim 2 \times 10^{-6}$ Torr on the O_2 pressure. Additional increases in O_2 pressure above this value would likely continue to shift the hump into the spike, significantly increasing the latter but making the two indistinguishable.

The companion ISOMS signals for isobutane and TMAA are shown in Figs. 2 and 3, respectively. The isobutane ISOMS profiles also exhibited changes as a function of increased O_2 pressure, but in different way than that observed for isobutene. The maximum isobutane ISOMS rate was not observed on initial exposure of the surface to UV, as was seen for isobutene. Instead, the maximum isobutane ISOMS rate was typically delayed by about 10–15 s from the start of UV irradiation, and the onset rate (at time 0) was approximately the same for all O_2 pressures explored. The general profile of the isobutane ISOMS traces changed as the O_2 pressure was increased, especially for pressures above 1×10^{-8} Torr. Instead of the rate acceleration effect observed for isobutene (Fig. 1), the isobutane rate decayed to zero more rapidly as the O_2 pressure was increased. For example, whereas the rate of isobutane evolution was still measurable after 300 s of UV irradiation in UHV,

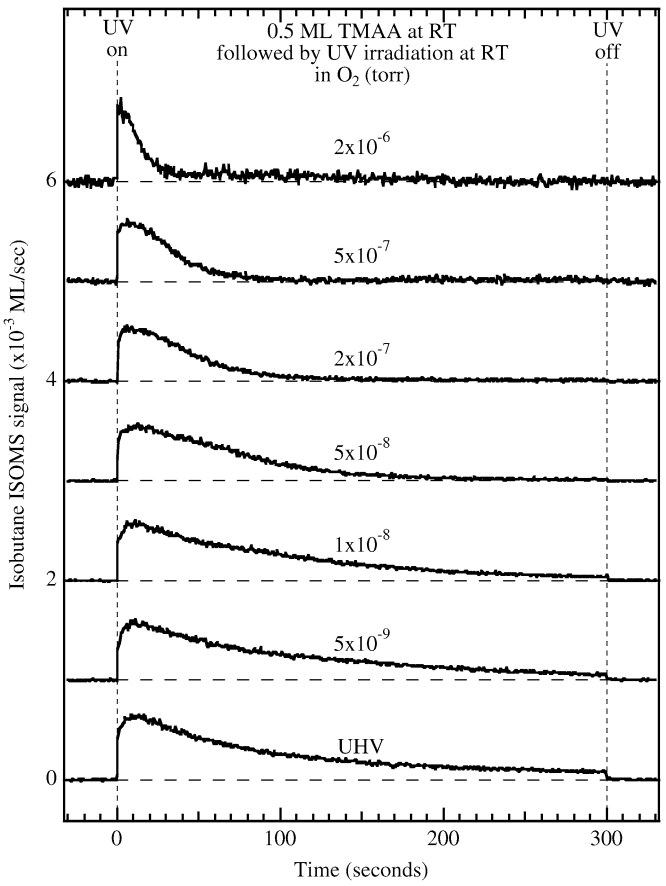

Fig. 2. Isobutane ISOMS scans from UV irradiation of 0.5 ML TMA on TiO_2(110) at RT in various background pressures of O_2. UV irradiation was commenced at time 0 s and was terminated at time 300 s. UV irradiation was with a 100 W Hg lamp. Spectra are displaced vertically and provided with background lines for clarity.

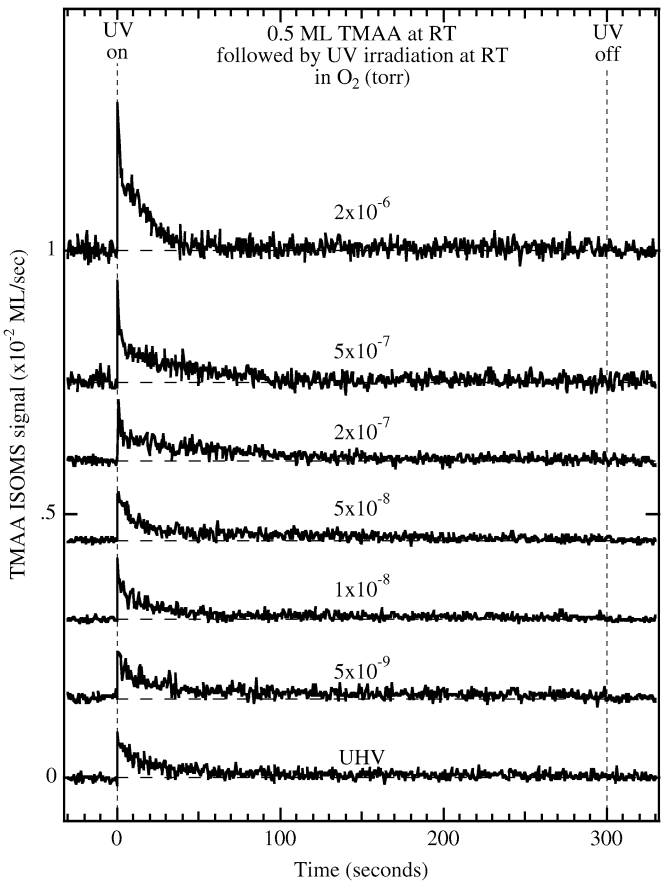

Fig. 3. TMAA ISOMS scans from UV irradiation of 0.5 ML TMA on TiO_2(110) at RT in various background pressures of O_2. UV irradiation was commenced at time 0 s and was terminated at time 300 s. UV irradiation was with a 100 W Hg lamp. Spectra are displaced vertically and provided with background lines for clarity.

the rate attenuated to near zero after 150 s in 2×10^{-7} Torr O_2 and after about 50 s in 2×10^{-6} Torr O_2. This effect was not strictly a factor of consumption of the available TMA groups, because the isobutene ISOMS rate persisted beyond the points at which the isobutane rates had attenuated. These data show a marked change in the selectivity of TMA photodecomposition as a function of both O_2 pressure and the extent of reaction.

In general, the TMAA ISOMS signals (Fig. 3) were weaker than the isobutene and isobutane signals but for the most part mirrored the isobutene signal in the spike region, although not in the hump region. The maximum TMAA ISOMS rates were consistently at the onset of UV irradiation irrespective of the O_2 pressure, and the rate generally attenuated to near zero after about 50–100 s of UV exposure.

There was no evidence in these studies for appreciable amounts of other hydrocarbon products, such as *t*-butanol, 2,2,3,3-tetramethylbutane (from dimerization of two *t*-butyl groups) or C_3 products, although some of these species were found in trace quantities in postirradiation TPD [9]. Therefore, a discussion of how O_2 pressure (and TMAA coverage, see below) influenced the reaction mechanism of TMA photodecomposition on TiO_2(110) at RT can be restricted to the isobutene, isobutane, and TMAA products.

The TMA adlayers probed under UHV conditions were prepared on surfaces with about 7–10% oxygen vacancy sites, with each of these sites occupied by what can nominally be considered as two trapped electrons in the form of Ti^{3+} centers (see [23] for more details on the nature of these sites). Because no O_2 was provided to scavenge either the photoexcited electrons or to react with the negative charge associated with the surface oxygen vacancies, there was the potential for consider accumulation of negative charge on the surface during photon irradiation. The total amount of TMA photodecomposition in the 5-min UV irradiation period in UHV was about 0.32 ML. It is unclear whether the excited electrons associated with the holes that had this level of TMA decomposition were trapped on the surface, trapped in the bulk, or conducted to ground through the sample holder. As we show below, the rate of the TMA photodecomposition reaction was considerably faster if the surface oxygen vacancies were oxidized before TMAA adsorption and UV irradiation in UHV.

Fig. 4 illustrates the changes in the selectivity of TMA photodecomposition as a function of O_2 pressure for an initial TMA coverage of 0.5 ML. The selectivity between isobutene and isobutane is expressed as the fractional yield of isobutene ($f_{ene} \equiv$ isobutene ISOMS signal divided by the sum of the

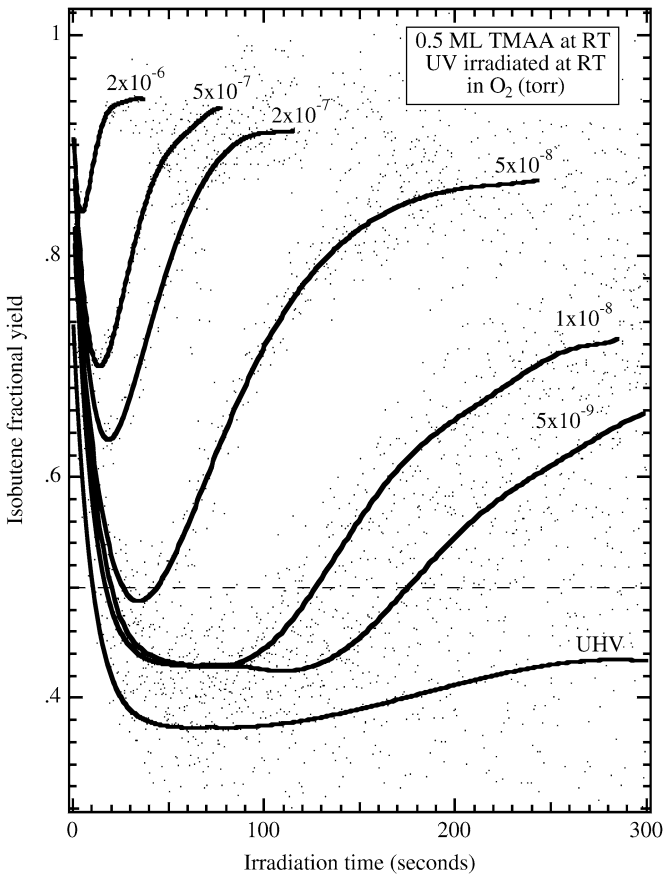

Fig. 4. Isobutene fractional yield curves obtained from the isobutene and isobutane ISOMS data in Figs. 1 and 2. Dots represent the raw data and lines represent least-squares polynomial fits to the data (provided for guiding the eye). The horizontal dashed line corresponds to a 1:1 ratio of isobutene-to-isobutane.

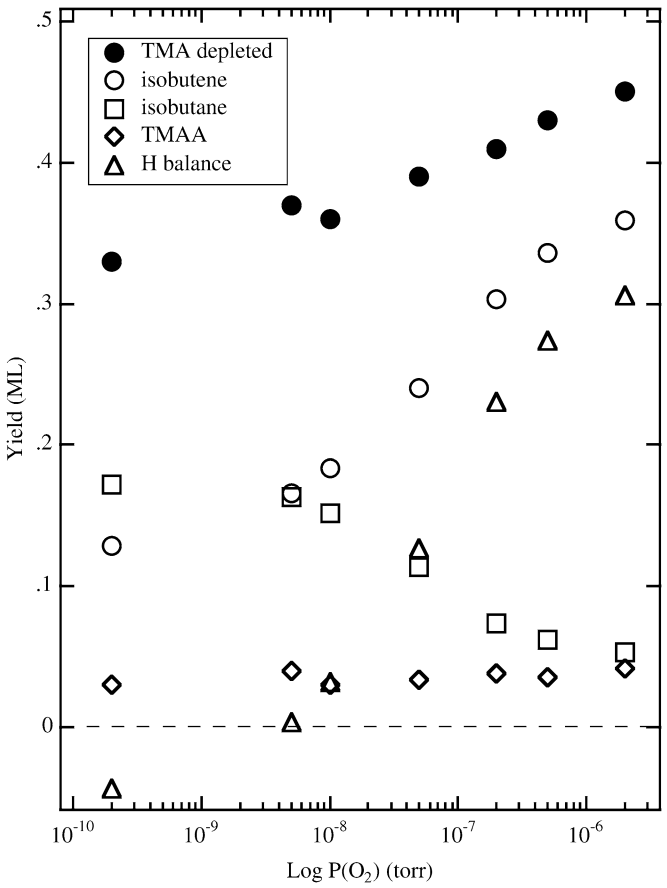

Fig. 5. Total yields as a function of the O_2 reaction pressure during the 5 min UV irradiation periods shown in Figs. 1–3 for isobutene (open circles), isobutane (open squares) and TMAA (open diamonds). The total amount of TMA depleted by UV irradiation (closed circles) was obtained from summation of these three yields. The H balance (open triangles) was obtained from substraction of the isobutane yield from the isobutene yield.

isobutene and isobutane ISOMS signals). The traces in this figure represent not the total yields seen at the end of the UV exposures (see Fig. 5 for discussion of these data), but how the yields changed as the reaction progressed. A value of 1 represents 100% selectivity to isobutene, and the horizontal dashed line at 0.5 signifies a 1:1 ratio of isobutene to isobutane. The dots are the raw data, which by nature of the plot exhibited significant noise as photodecomposition of the TMA adlayer approached completion. The solid traces represent least squares polynomial fits to the data and are presented only to guide the eye. Completion was approached more rapidly at high O_2 pressures, so the fitted lines extend to longer times at lower O_2 pressures.

Examination of the f_{ene} values shows that the initial selectivity of the TMA photodecomposition reaction was toward isobutene, due largely to the spikes of isobutene at the start of each UV experiment (see Fig. 1). The initial f_{ene} was consistently >0.7, but was higher at higher O_2 pressures. As the reaction proceeded in each case, the selectivity shifted toward a greater contribution of isobutane, but then reverted back toward isobutene in the latter stages of the reaction. In addition, the minimum in the isobutene selectivity moved to longer times for lower O_2 pressures. Interestingly, the minimum in each case occurred after $13 \pm 2\%$ of the surface TMA was converted to isobutene. The different f_{ene} values at these minima therefore reflect changes in the isobutane yields. For example, in the 2×10^{-6} Torr O_2, case the minimum f_{ene} occurred after 2% conversion of TMA to isobutane and 11% conversion to isobutene. In 5×10^{-8} Torr O_2, the conversions to isobutane and isobutene at the minimum were 8 and 13%, respectively. In the UHV case, placing the minimum at 60 s corresponds to relative yields of isobutane and isobutene of 20 and 12%, respectively. In this case, the isobutene-to-isobutane ratio dropped below 1:1 from a point 15 s into the reaction and stayed below this level for the remainder of the reaction. Similarly, the isobutene to isobutane ratio dropped below 1:1 in the O_2 pressure range between 5×10^{-9} and 5×10^{-8} Torr but eventually rose above 1:1, with the time period persisting below this ratio decreasing as the O_2 pressure increased. These data suggest that the extent of hydrogenation (isobutane production) versus partial oxidation (isobutene production) of the *t*-butyl radical depends on the O_2 pressure and the adsorbate coverage on the surface. This observation is discussed in more detail below.

Fig. 5 shows the total ISOMS yields for isobutene (open circles), isobutane (open squares), and TMAA (open diamonds) as a result of the 5-min irradiation periods used in obtaining the

data shown in Figs. 1–3. Along with these yields are shown the total amount of TMA depleted from the surface due to UV exposures (filled circles) and the hydrogen balance affected by the isobutene-to-isobutane selectivity (open triangles). All of these values are plotted versus the log of the O_2 pressure, with the assumption that the O_2 partial pressure under UHV conditions was no greater than 2×10^{-10} Torr. The total amounts of TMA depleted during the 5-min irradiation periods were obtained by subtracting the summed ISOMS yields of isobutene, isobutane, and TMAA from the initial TMAA coverage. These values were consistent with the amount of TMAA dosed in each case (0.5 ML) and the amounts of unreacted TMA left on the surface after termination of UV irradiation, as probed by TPD (data not shown). The amount of depleted TMA increased linearly with the log of the O_2 pressure, but the amount of TMAA photodesorbed was small and roughly constant as a function of increasing O_2 pressure. The total yields of isobutene and isobutane were approximately equivalent for O_2 pressures below about 1×10^{-8} Torr, but the amount of isobutene increased and the amount of isobutane decreased as the O_2 pressure was increased above this level. Because of this change, the H balance on the surface shifted. The open triangles in Fig. 5 reflecting the H balance were obtained from the amount of isobutene produced minus the amount of isobutane produced. Although the data in Fig. 4 show that the isobutene-to-isobutane ratio was not steady at 1:1 under any conditions in this study, the UHV case most closely provided a stoichiometric situation such as that represented in reaction (5). The imbalance could arise from the existence of one or more competing reactions that altered the overall isobutene-to-isobutane ratio away from 1:1.

To form isobutene, a H atom must be removed from one of the methyl groups of the *t*-butyl radical,

$$t\text{-Butyl}_{(a)} \rightarrow i\text{-}C_4H_{8(g)} + H_{(a)}. \quad (6)$$

Conversely, a H atom must be added to the tertiary C of the *t*-butyl radical in order to form isobutane,

$$t\text{-Butyl}_{(a)} + H_{(a)} \rightarrow i\text{-}C_4H_{10\,(g)}. \quad (7)$$

If these processes were concerted (e.g., in the disproportionation reaction) or otherwise offset each other, then the H balance would remain at zero; that is, there would be no deposition of H or need for additional H. In UHV, there was a small imbalance toward H being required because the total amount of isobutane exceeded that of isobutene. This could indicate that some of the acid protons deposited on the surface from TMAA dissociation adsorption were used or that a slight error exists in the calibrations of the isobutene and isobutane yields. As the O_2 pressure was increased, the H balance shifted toward deposition of H on the surface because more isobutene was produced than isobutane. TPD after ISOMS (not shown) did not provide evidence for surface accumulation of H in any form (e.g., OH, or adsorbed water) during UV irradiation in O_2 pressures above 1×10^{-8} Torr; however other ISOMS data (not shown) suggest that water slowly evolved from the surface during UV irradiation. These data are not conclusive, however, due to the low signal-to-noise resulting from high water background signals caused by backfilling the chamber with oxygen. As discussed previously, O_2 reacts with OH groups bound to Ti^{3+} sites, resulting in both H atom abstraction from the OH group and oxidation of the Ti^{3+} [reaction (4)] [6,16]. Post-irradiation TPD (not shown) reveals that most of the OH groups formed from dissociative adsorption of the acid on the surface have been reacted with O_2 at RT to generate and desorb water, consistent with previous results [16,20].

Changes in the isobutene versus isobutane selectivity as a function of O_2 pressure coincide with a structural change in the TMA adlayer as revealed by the STM images in Fig. 6. (In each image, the Ti^{4+} rows run from the upper left of the lower right.) Fig. 6a shows the STM image of the TMA-saturated surface. The TMA adlayer consists of a highly ordered (2×1) structure. (Large white spots were impurities present on the surface at ∼0.01 ML level.) The three images in Fig. 6b–d represent UV irradiation (in this case with a 300 W Xe lamp; see the Experimental section) of a saturation coverage of TMA at 280 K in UHV for 1 h (b), in 1×10^{-7} Torr O_2 for 15 min (c), and in 1×10^{-6} Torr O_2 for 5 min (d). (Images were collected at 280 K to minimize TMA surface diffusion.) The TMA photoproducts (CO_2, isobutene, and isobutane) desorb from the surface at RT, leaving unoccupied sites. Therefore, evidence for photodecomposition of TMA in STM comes from empty sites or groups of sites that appear after irradiation in the otherwise completely TMA-covered surface. The extent of photodecomposition of the saturated TMA surface can be judged by either the number of remaining TMA groups or on the number of empty sites. The purpose of the STM data in Fig. 6 is not to provide an approximate amount of TMA photodecomposition (although this can be done by counting), but rather to show that the distribution of single empty sites versus clusters of empty sites (“voids”) changed as a function of the O_2 pressure. Under UHV conditions, UV irradiation for 1 h yielded a TMA overlayer in which about 66% of the TMA groups were removed (0.17 ML left from the initial 0.5 ML). The distributions of empty sites and remaining TMA groups were fairly random, implying that each photodecomposition event occurred more or less independently from previous events or remaining (unreacted) TMA groups. (The dark areas in the top right and bottom middle of the image are from a lower terrace, and the dark region in the upper left is from a small pit in the terrace similar to those in the terrace on the right side of the image in Fig. 6a.)

Fig. 6c shows the STM image collected after 15 min of UV irradiation in 1×10^{-7} Torr O_2 of a saturated TMA adlayer on TiO_2(110). The extent of the photodecomposition reaction in this case was about $55 \pm 5\%$, which translates into an unreacted TMA coverage of about 0.23 ML. The unreacted TMA groups were not randomly distributed across the surface as was observed for the UHV case (Fig. 6b). Voids in the TMA adlayer existed in which the local coverage of TMA was <0.1 ML. In addition, features were resolved inside these voids that were previously assigned to OH and/or O_x species [6–8]. There was also evidence in the image of Fig. 6c for homogeneous removal of TMA in areas away from the voids. This suggests that at low O_2 pressures, the kinetics for homogeneous removal of TMA compete well with void formation. As discussed previously [7], the appearance and growth of the void regions matches the rate

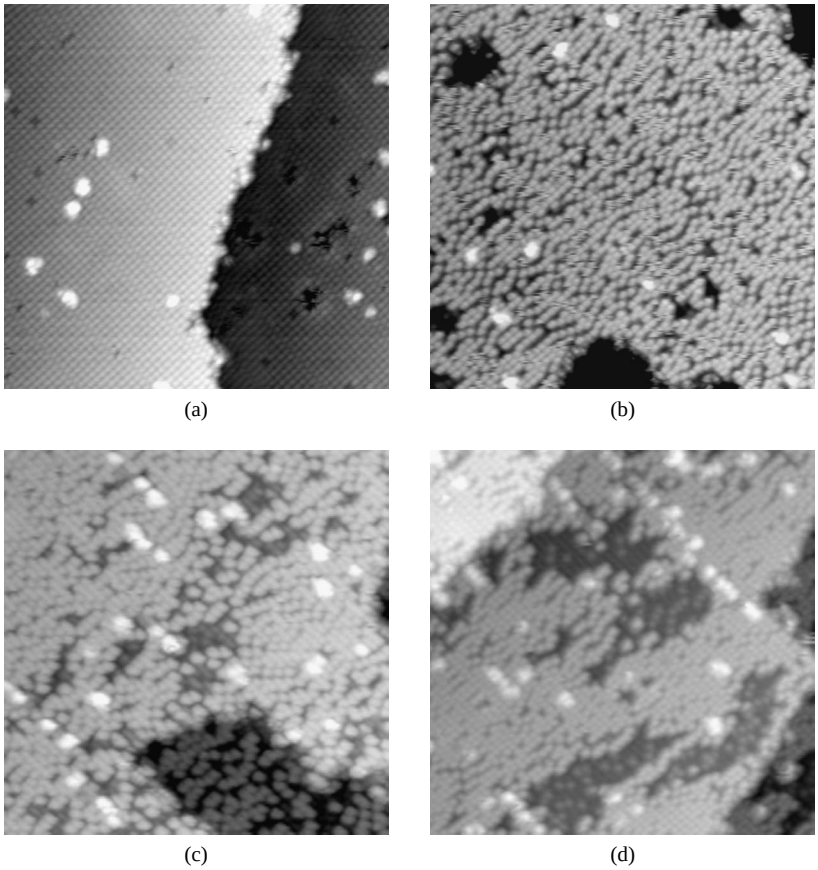

Fig. 6. STM images from (a) a saturation coverage of TMA on TiO_2(110), (b) UV irradiation of 'a' in UHV for 1 h, (c) UV irradiation of 'a' in 1×10^{-7} Torr O_2 for 15 min, and (d) UV irradiation of 'a' in 1×10^{-6} Torr O_2 for 5 min. Each image is nominally 31×31 nm^2, and obtained using a sample bias of +1.3 to +1.6 V and tunneling current of ∼0.4 nA. UV irradiation was with a 300 W Xe lamp.

acceleration seen in the isobutene ISOMS signals (Fig. 1) and hence the point at which the selectivity shifts from the minimum in the isobutene-to-isobutane ratio to preferential production of isobutene.

To further illustrate the spatial inhomogenity of the TMA photodecomposition reaction on TiO_2(110) in a background of O_2, the STM image of Fig. 6d shows the distribution of TMA groups remaining after 5 min of UV irradiation of a saturated TMA adlayer in 1×10^{-6} Torr O_2. In this case, the extent of reaction was also about 50%, but in contrast to the image obtained in 1×10^{-7} Torr O_2 (Fig. 6c), the void regions were larger and the surface coverage in the TMA-rich regions was greater than in the 1×10^{-7} Torr O_2 case. (Note also that the reaction time required to reach 50% depletion decreased significantly with increasing O_2 pressure.) The voids did not adopt a uniform shape, but had irregular borders between TMA-rich and OH/O-rich areas of the surface. Under these conditions, the selectivity of the reaction significantly shifted toward isobutene, and the rate of reaction accelerated as the selectivity shifted.

Taken together, the data in Figs. 1–6 show a correlation between the selectivity of TMA photodecomposition and the degree of spatial homogeneity in which the reaction proceeds on the surface. These data also suggest that two experimental parameters play determining roles in the selectivity of TMA photodecomposition on TiO_2(110) at RT. The most obvious factor is the influence of O_2. Data in Figs. 7–12 show that TMA coverage is also an important factor.

3.2. Effect of TMA coverage

Figs. 7–9 show ISOMS data for isobutene, isobutane, and TMAA, respectively, during UV irradiation of various initial coverages of TMA on TiO_2(110). For these experiments, a background O_2 pressure of 5×10^{-7} Torr was used to ensure detectable ISOMS signals at low TMA coverages as well as conditions in which void formation was favorable. Fig. 7 shows isobutene ISOMS traces for various initial coverages of TMA photolyzed in 5×10^{-7} Torr O_2. There was no sign of acceleration in the isobutene ISOMS rate indicative of void formation for initial TMA coverages <0.28 ML. Instead, the maximum rate was observed immediately on exposure of the surface to UV, with the rate attenuating rapidly thereafter. The intensity of the initial spike and the amount desorbed did not scale with the TMA coverage, as discussed below. Evidence for void formation and rate acceleration were evident in the "hump" observed in the latter stages of the photolysis experiment for coverages above ∼0.28 ML. In contrast to these isobutene ISOMS results, very little isobutane (Fig. 8) or TMAA (Fig. 9) ISOMS signal were detected at the lowest TMA coverage probed (0.05 ML). The small amounts of

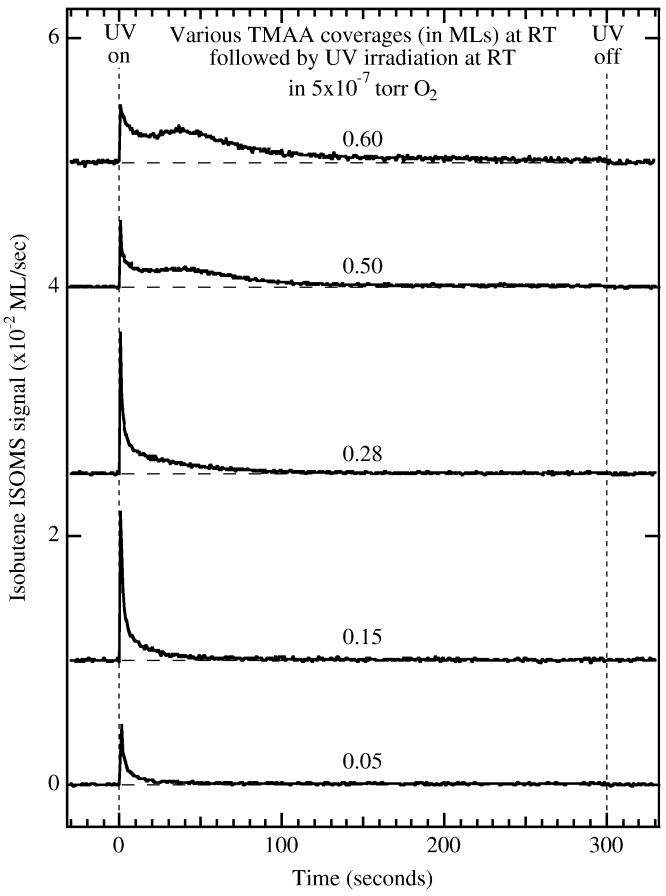

Fig. 7. Isobutene ISOMS scans from UV irradiation of various coverages of TMA on TiO_2(110) at RT in 5×10^{-7} Torr O_2. UV irradiation was commenced at time 0 s and was terminated at time 300 s. UV irradiation was with a 100 W Hg lamp. Spectra are displaced vertically and provided with background lines for clarity.

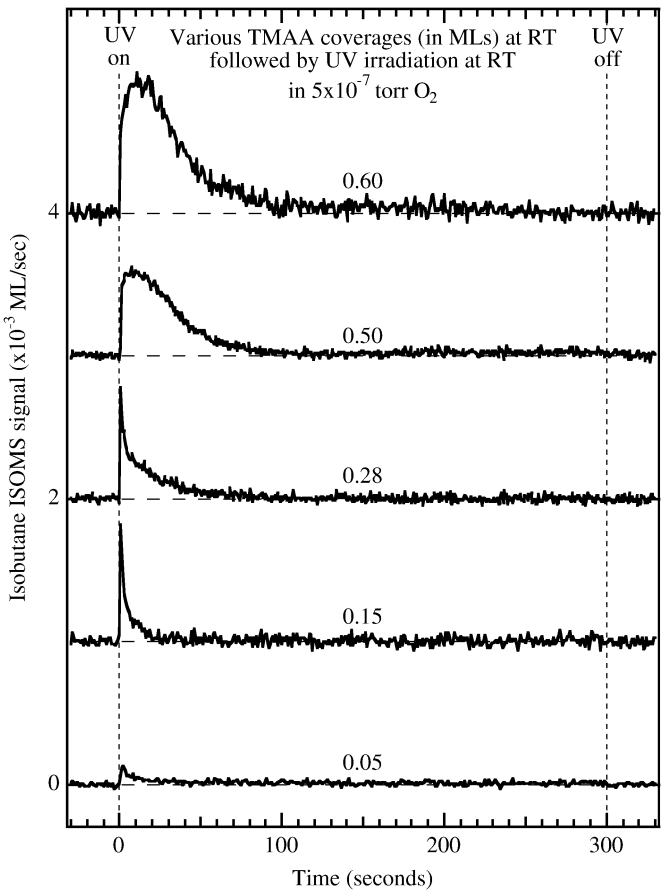

Fig. 8. Isobutane ISOMS scans from UV irradiation of various coverages of TMA on TiO_2(110) at RT in 5×10^{-7} Torr O_2. UV irradiation was commenced at time 0 s and was terminated at time 300 s. UV irradiation was with a 100 W Hg lamp. Spectra are displaced vertically and provided with background lines for clarity.

isobutane detected as the initial TMA coverage was increased evolved predominantly in the spike region. The spike persisted in the isobutane ISOMS signal for initial TMA coverages up to at least 0.28 ML, but above this point the spike decreased and the isobutane ISOMS profile evolved into the shape and characteristics seen for high TMA coverages irrespective of the O_2 pressure (Fig. 2). The TMAA ISOMS signals retained a maximum rate in the spike but developed a tail in the rate as the initial coverage of TMA was increased.

As was done for the isobutene and isobutane ISOMS data in Fig. 4, Fig. 10 shows the fractional yield of isobutene during the course of the photodecomposition reactions probed in Figs. 7 and 8. At low initial TMA coverages, the isobutene yield remained >90% throughout the reaction. The isobutene yield decreased slightly as the initial TMA coverage was increased to 0.15 ML. Evidence for the rate acceleration effect, as revealed by a minimum in the isobutene yield followed by a shift toward more isobutene, was seen at an initial TMA coverage of 0.28 ML. The fractional yield curves for 0.5 and 0.6 ML TMA were nearly identical.

In the case of the 0.05 ML initial TMA coverage, near-100% conversion of the adsorbed TMA was achieved after about 50 s of UV light (see filled circles in Fig. 11), but the conversion percentage during the 5-min irradiation period dropped to 56% as the initial TMA coverage was increased to 0.15 ML. The conversion decreased linearly with increasing initial TMA coverage between 0.15 and 0.5 ML, as shown in Fig. 11. This decrease in conversion can be attributed to one of two effects. First, whereas the conditions in the 0.05 ML case may have been ideally balanced in terms of the fluxes of light and O_2 to achieve ∼100% conversion in 50 s, an increase in TMA coverage might have placed the reaction in a flux-limited situation with regards to UV light and/or O_2. But this does not appear to be the case, for two reasons: (1) The rates of TMA photodecomposition in the two cases (0.05 and 0.15 ML TMA) were approximately the same, indicating the absence of a flux limitation in the first 20 s of the reaction, and (2) achieving ∼100% selectivity in a flux-limiting situation should only require the reaction time to be scaled by the coverage increase (a factor of 3). This was not observed since only 56% conversion was reached by a six-fold increase in the reaction time (i.e., from 50 s for ∼100% conversion in the 0.05 ML case to 300 s to reach only 56% conversion in the 0.15 ML case).

The second possibility, supported by STM, suggests that the TMA photodecomposition probability is affected by TMA–TMA interactions. STM images in Fig. 12 correspond to initial

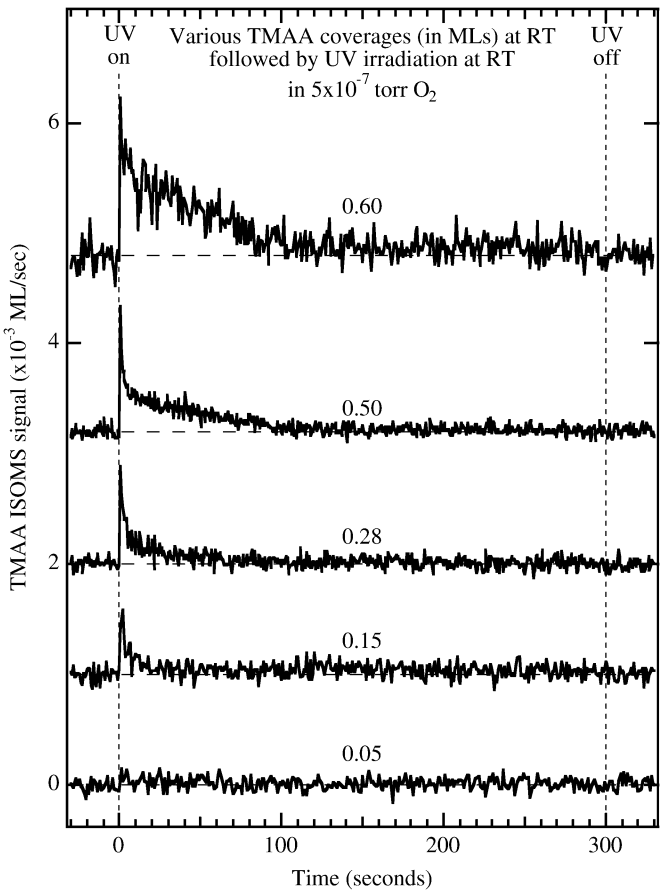

Fig. 9. TMAA ISOMS scans from UV irradiation of various coverages of TMA on TiO_2(110) at RT in 5×10^{-7} Torr O_2. UV irradiation was commenced at time 0 s and was terminated at time 300 s. UV irradiation was with a 100 W Hg lamp. Spectra are displaced vertically and provided with background lines for clarity.

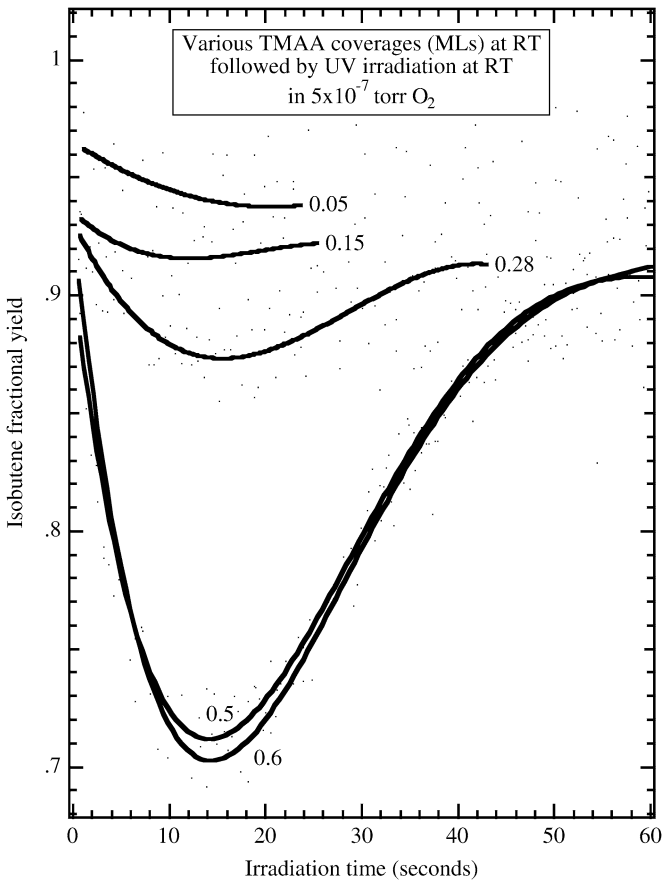

Fig. 10. Isobutene fractional yield curves obtained from the isobutene and isobutane ISOMS data in Figs. 8 and 9. Dots represent the raw data and lines represent least-squares polynomial fits to the data (provided for guiding the eye).

TMA coverages at 280 K on TiO_2(110) between 0.014 and 0.13 ML. In each case, the clean surface (which had ∼10% O vacancies) was exposed to 200 L O_2 at RT before TMAA adsorption. Although this adsorption order was switched in the ISOMS data of Figs. 7–9, the surfaces in the latter saw ∼120 L O_2 between the adsorption of TMA and the commencement of UV irradiation because the O_2 pressure (5×10^{-7} Torr) was typically stabilized for 4 min before UV irradiation. These conditions are comparable as long as the TMA coverage was low based on ISOMS data in which the TMAA and O_2 adsorption order was switched (data not shown). The bright spots in Fig. 12 were due to TMA groups, and the faint spots (also on the Ti^{4+} rows) were due to O_x species [20,24,25]. At the lowest coverage (0.014 ML; Fig. 12a), the TMA groups were isolated from each other, and very few occupied adjacent surface unit cells in either surface direction (along or across the Ti^{4+} row direction). This situation was maintained when the coverage was near doubled to 0.026 ML (Fig. 12b), although some TMA groups formed pairs along the <1$\bar{1}$0> direction. The presence of O_x species on the Ti^{4+} sites did not appear to prevent TMA–TMA interactions along the <001> direction because there were a number of incidents in the image of Fig. 12b in which no faint spots separated TMA groups along this direction and yet TMA–TMA pairings did not form. This is because carboxylates tend to repel each other on TiO_2(110) along the <001> direction [22,26].

A significant change in the ordering of TMA did occur when the coverage was increased by an additional factor of 5 (from 0.026 to 0.13 ML). Although there were still numerous isolated TMA groups at a 0.13-ML coverage, a significant number participated in forming linear chains along the <1$\bar{1}$0> direction. The ordering in this direction is believed to be facilitated by the deposition of acid protons (residing on the bridging O^{2-} rows), which screen and align adjacent carboxylates [26]; similar ordering has been observed with other carboxylates on TiO_2(110) [22]. Comparing the ISOMS data in Figs. 7–9 with the STM images in Fig. 12 suggests that the rate of TMA photodecomposition on TiO_2(110) was influenced by whether or not TMA–TMA interactions existed. We speculate that the reaction probability of a TMA group in a TMA-OH–TMA pairing (where the OH refers to a bridging OH located on the rows of bridging O^{2-} sites, formed from dissociation of the TMAA O–H bond) with a hole in the TiO_2 valence band is less than that with an isolated TMA group. Whether electrostatics inhibit approach of the hole, or whether the bridging OH group becomes a trap site for an excited electron and, consequently, a recombination center for an approaching hole, cannot be determined from these data.

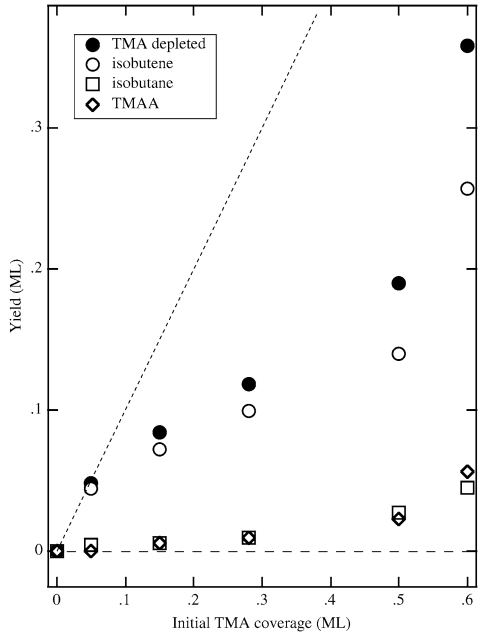

Fig. 11. Total yields as a function of TMA coverage during the 5 min UV irradiation periods shown in Figs. 8–10 for isobutene (open circles), isobutane (open squares) and TMAA (open diamonds). The total amount of TMA depleted by UV irradiation (closed circles) was obtained from summation of these three yields. The dashed line represents 100% conversion of the initial TMA coverage to product (e.g., isobutene).

Fig. 12c also shows the beginning signs of establishment of order along the <001> direction as <1$\bar{1}$0>-oriented lines of TMA groups are forced to accommodate with each other. The reaction selectivity of the resulting *t*-butyl radical does not shift from isobutene toward an isobutene and isobutane mixture unless the initial coverage is higher than that probed in Fig. 12. Therefore, the changes in selectivity appear to arise not from TMA–TMA interactions along the <1$\bar{1}$0> direction, but rather from increasing TMA–TMA interactions along the <001> direction, where TMA groups come into adjacent sites along the rows of Ti^{4+} sites. This coincides with isobutane selectivity becoming more pronounced as the coverage was increased above 0.28 ML (Fig. 10). A possible mechanism for this is the reaction of a *t*-butyl group with a TMA group to form isobutene and isobutane,

$$t\text{-Butyl}_{(a)} + \text{TMA}_{(a)} \rightarrow i\text{-}C_4H_{8(g)} + i\text{-}C_4H_{10(g)} + CO_{2(g)}. \quad (8)$$

A complication with this reaction is that at saturation coverages the photoreaction initially favors isobutene over isobutane (see Fig. 10), but this may be because there are few available sites for the *t*-butyl group to adsorb, so the *t*-butyl group unimolecularly decomposes to isobutene via H-atom transfer to the surface.

Although the isobutene fractional yield profile did not change much when the coverage was increased from 0.5 to 0.6 ML (Fig. 10), the total conversion during the 5-min UV irradiation period significantly increased from ∼38% for the 0.5 ML case to 60% for the 0.6 ML case (Fig. 11). This increased conversion might be interpreted as resulting from the rate being sensitive to coverage. The difference between the degree of intermolecular repulsion at a coverage of 0.5 ML

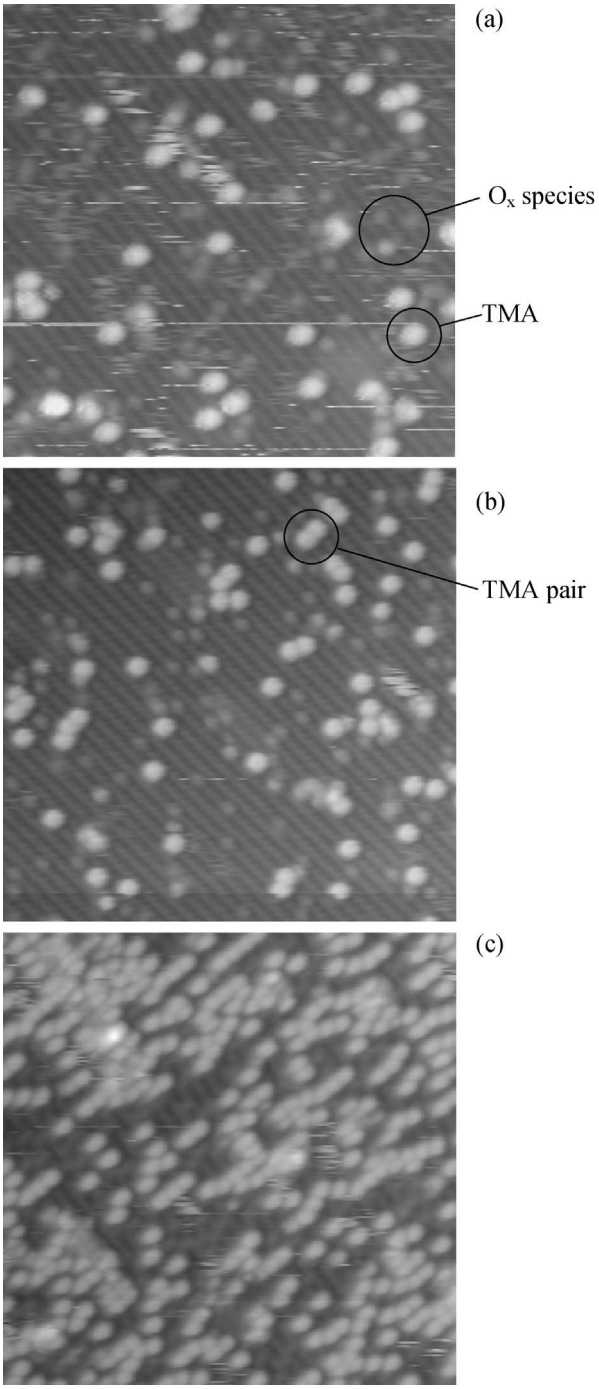

Fig. 12. STM images from (a) 0.014 ML, (b) 0.026 ML and (c) 0.13 ML of TMA on TiO_2(110) surface. In each case, the surface was dosed with 200 L O_2 at RT prior to TMAA adsorption. Each image is nominally 21 × 21 nm^2, and obtained using a sample bias of +1.3 to +1.6 V and tunneling current of ∼0.4 nA.

(one TMA per every two Ti^{4+} sites) and 0.6 ML (three TMAs per every five Ti^{4+} sites) should be significant; however, increased repulsions between 0.15 and 0.5 ML TMA decreased the conversion. The isobutene and isobutane ISOMS profiles for the two coverages (0.5 and 0.6 ML) were similar (Figs. 7 and 8), as were the isobutene fractional yield curves (Fig. 10). The difference in conversion between the two highest coverages may instead have arisen from a structural difference

between the two adlayers of these coverages. A likely source of the selectivity difference between 0.5 and 0.6 ML TMA may have been due to the presence of some η^1-TMA in the 0.6-ML surface. Ideally, a 0.5-ML coverage of TMA would comprise all η^2-TMA groups bridge-bonded between adjacent Ti^{4+} sites along the surface's <001> direction. For the coverage to exceed 0.5 ML, some η^2-TMA groups must convert to η^1-configurations, where the TMA is bound to a single Ti^{4+} site through a single *t*-BuC(=O)–O–Ti linkage. To achieve a 0.6-ML TMA coverage, approximately 0.2 ML of TMA must be adsorbed in the η^1-configuration. The η^1-configuration has been observed for high coverages of carboxylates on TiO_2(110) using STM [27]. In those STM experiments, because of long data acquisition times, a constant flux of carboxylic acid was maintained on the surface to keep the surface saturated. In the ISOMS experiments, the time between dosing and data collection was typically short (no longer than minutes), so high coverages dosed at RT could be probed without significant loss of coverage due to slow thermal desorption. On the other hand, as much as 10% of the initial TMA coverage was lost to vacuum at RT by holding the as-dosed surface at RT for 20 min before data acquisition (data not shown). Therefore, the surface corresponding to the STM image in Fig. 6a likely did not have much η^1-TMA. Another situation in which η^1 carboxylates are observed is when the surface cation–cation site distance is too large for η^2 species to form a bridge. This is not the case for TiO_2(110), but has been observed for formate on rutile TiO_2(111) [28]. The possibility that η^1 carboxylates are more photoreactive to holes in TiO_2 than are η^2 carboxylates suggests that the structure of the TiO_2 crystal face is important. Surfaces in which η^1-carboxylates dominate [e.g., TiO_2(111)] may show higher photocatalytic activity for oxidation of carboxylic acids.

3.3. Effect of surface preoxidation

The TMA adlayers used in the photooxidation experiments of Figs. 7–9 were, by necessity, exposed to O_2 before irradiation with UV. The O_2 preexposure period was not important for saturation coverages of TMA, because no adsorption sites for O_2 were available until a TMA photodecomposition event had occurred. However, at lower TMA coverages, it is important to consider what effect, if any, O_2 adsorption before UV irradiation might have had on the photooxidation process. Fig. 13 shows ISOMS data for isobutane, isobutene, TMAA, and water from a saturation coverage of TMA adsorbed on TiO_2(110) that was predosed with 15 L of O_2 at RT. In this case, UV irradiation was conducted in UHV after dosing TMAA. The data show spikes in the isobutane, isobutene, and TMAA signals on exposure to UV, each decaying away with irradiation time. Even though the photolysis was conducted in UHV, where the isobutene-to-isobutane ratio would otherwise be nearly 1:1 (see Fig. 4), the preadsorbed O_x species enhanced the initial isobutene yield to >90% and sustained the overall selectivity of the reaction at >65% isobutene at any given moment during the reaction (see the dots at the bottom of Fig. 13). Although little or no water was detected (see the top trace of Fig. 13), an

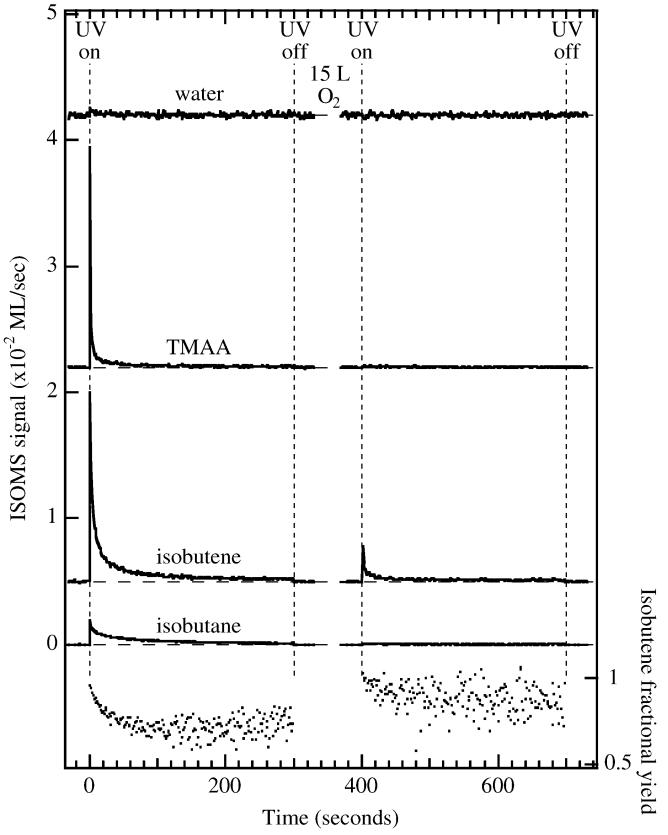

Fig. 13. ISOMS scans for water, TMAA, isobutene and isobutane from UV irradiation of a saturation TMA coverages on TiO_2(110). The surface was dosed with 15 L O_2 at RT prior to TMAA adsorption. UV irradiation was commenced at time 0 s and was interrupted at time 300 s, at which point the surface was exposed to an additional 15 L O_2. UV irradiation was then recommenced. (UV start time for the second UV irradiation period was shifted on the *x*-axis to 400 s.) UV irradiation was with a 100 W Hg lamp. Spectra are displaced vertically and provided with background lines for clarity. Dots in the lower portion of the figure are the isobutene fractional yields.

unusually sharp and intense TMAA spike was observed on exposure of the surface to UV. The TMAA spike decayed more rapidly than did the spikes of isobutene or isobutane. Such intense TMAA spikes in ISOMS were detected only when the surface was preoxidized and a saturation coverage of TMAA followed. Note that reexposure of this surface to 15 O_2 after the initial 5-min photolysis period resulted in additional (although smaller) isobutene and isobutane production, but with little or no TMAA or water signal when subsequently irradiated with UV in UHV. TPD after the ISOMS experiments of Fig. 13 (not shown) indicated that more than half of the initial TMA coverage was unreacted and that virtually all of the initial coverage of H from the acid dissociation still resided on the surface. The H balance appeared to be made up through TMAA production according to the following reaction:

$$2\mathrm{TMA}_{(a)} + h\nu \rightarrow i\text{-}\mathrm{C_4H_{8(g)}} + \mathrm{CO_{2(g)}} + \mathrm{TMAA_{(g)}}. \quad (9)$$

Keeping in mind that intense TMAA desorption was observed only with preadsorbed O and a saturation coverage of TMA, and only on initial exposure to UV light, the mechanism may involve an η^1-TMA group as one of the two TMA groups. This would explain the rapid decay for the TMAA ISOMS signal

as the high coverage situation (which favors η^1-TMA) was relieved by TMA photodecomposition. However, the need for the preadsorbed O_x species is not understood.

The preoxidation data show that the presence of adsorbed O_x species increased the initial TMA photodecomposition rate, but the rate decayed as the influence of the O_x species was dissipated. We have previously speculated that preadsorption of O_2 titrates electron density associated with oxygen vacancies, permitting an initially fast reaction until the coverage of trapped electrons increased and inhibited hole-related processes [6–8]. It also appears that preadsorbed O_x species shifted the isobutene-to-isobutane ratio toward isobutene and promoted TMAA photodesorption.

4. Conclusion

We have shown that the selectivity of TMA photodecomposition on TiO_2(110) is sensitive to both the O_2 pressure and the initial coverage of TMA. The TMA-covered surface forms a well-ordered (2×1) array of TMA groups. The first photodecomposition event in this saturated array results in a spike of CO_2 and isobutene (i-C_4H_8) desorption, presumably with the retention of a H atom on the surface. Because the surface is saturated, the selectivity in this first step in the reaction is relatively insensitive to the O_2 pressure. As photolysis is continued in UHV (no O_2), additional decomposition events open sites on the surface that permit the overall stoichiometry to favor a disproportion reaction of the resulting t-butyl groups to roughly a 1:1 mixture of isobutane (i-C_4H_{10}) to isobutene. This trend continues until the adlayer is depleted. Initially, the trend toward a 1:1 yield of isobutane to isobutene is also observed in an O_2 background, but as the number of unoccupied sites increases, void regions open in the TMA overlayer, facilitating O_2 adsorption, which accelerates the rate and shifts the selectivity toward isobutene. The reaction proceeds rapidly at the hydrophobic (TMA)–hydrophilic (OH) boundary on the surface until the reactant is consumed. These results illustrate both the changing dynamics of a typical photooxidation reaction on TiO_2 and also how the same factors that influence these dynamics (i.e., O_2 pressure and TMA coverage) cause changes in the selectivity of the photooxidation reaction.

Acknowledgments

M.A.H. and J.M.W. acknowledge support by the US Department of Energy, Office of Basic Energy Sciences, Division of Chemical Sciences. J.M.W. also acknowledges support from the Center for Materials Chemistry at the University of Texas at Austin and the Robert A. Welch Foundation. H.U. and H.O. acknowledge the support by Core Research for Evolutional Science and Technology by Japan Science and Technology Agency. Pacific Northwest National Laboratory is a multiprogram national laboratory operated for the US Department of Energy by the Battelle Memorial Institute under contract DEAC06-76RLO1830. Part of the research reported here was performed in the William R. Wiley Environmental Molecular Science Laboratory, a Department of Energy user facility funded by the Office of Biological and Environmental Research.

References

[1] M.A. Fox, M.T. Dulay, Chem. Rev. 93 (1993) 341.
[2] A.L. Linsebigler, G. Lu, J.T. Yates Jr., Chem. Rev. 95 (1995) 735.
[3] A. Mills, S. Le Hunte, J. Photochem. Photobiol. A 108 (1997) 1.
[4] A. Fujishima, T.N. Rao, D.A. Tryk, J. Photochem. Photobiol. C 1 (2000) 1.
[5] J.M. White, J. Szanyi, M.A. Henderson, J. Phys. Chem. B 107 (2003) 9029.
[6] M.A. Henderson, J.M. White, H. Uetsuka, H. Onishi, J. Am. Chem. Soc. 125 (2003) 14974.
[7] H. Uetsuka, H. Onishi, M.A. Henderson, J.M. White, J. Phys. Chem. B 108 (2004) 10621.
[8] J.M. White, M.A. Henderson, H. Uetsuka, H. Onishi, Proceedings of SPIE 5513 (Physical Chemistry of Interfaces, Nanomaterials III) (2004), p. 66.
[9] J.M. White, M.A. Henderson, J. Phys. Chem. B 109 (2005) 12417.
[10] J.M. White, J. Szanyi, M.A. Henderson, J. Phys. Chem. B 108 (2004) 3592.
[11] H. Hunsdiecker, C. Hunsdiecker, Ber. 75 (1942) 291.
[12] B. Kraeutler, A.J. Bard, J. Am. Chem. Soc. 100 (1978) 2239.
[13] B. Kraeutler, A.J. Bard, Nouv. J. Chim. 3 (1979) 31.
[14] S.H. Szczepankiewicz, A.J. Colussi, M.R. Hoffmann, J. Phys. Chem. B 104 (2000) 9842.
[15] S.H. Szczepankiewicz, J.A. Moss, M.R. Hoffmann, J. Phys. Chem. B 106 (2002) 2922.
[16] M.A. Henderson, W.S. Epling, C.H.F. Peden, C.L. Perkins, J. Phys. Chem. B 107 (2003) 534.
[17] Y. Nosaka, Y. Yamashita, H. Fukuyama, J. Phys. Chem. B 101 (1997) 5822.
[18] G. Liu, J. Zhao, H. Hidaka, J. Photochem. Photobiol. A 133 (2000) 83.
[19] H. Goto, Y. Hanada, T. Ohno, M. Matsumura, J. Catal. 225 (2004) 223.
[20] W.S. Epling, C.H.F. Peden, M.A. Henderson, U. Diebold, Surf. Sci. 412/413 (1998) 333.
[21] M.A. Henderson, Surf. Sci. 355 (1996) 151.
[22] H. Onishi, Springer Ser. Chem. Phys. 70 (2003) 75.
[23] U. Diebold, Surf. Sci. Rep. 48 (2003) 53.
[24] M.A. Henderson, W.S. Epling, C.L. Perkins, C.H.F. Peden, U. Diebold, J. Phys. Chem. B 103 (1999) 5328.
[25] R. Schaub, E. Wahlstroem, A. Ronnau, E. Laegsgaard, I. Stensgaard, F. Besenbacher, Science 299 (2003) 377.
[26] H. Onishi, K.-I. Fukui, Y. Iwasawa, Jpn. J. Appl. Phys., Part 1 38 (1999) 3830.
[27] H. Uetsuka, A. Sasahara, A. Yamakata, H. Onishi, J. Phys. Chem. B 106 (2002) 11549.
[28] H. Uetsuka, M.A. Henderson, A. Sasahara, H. Onishi, J. Phys. Chem. B 108 (2004) 13706.